Momentum-space analysis of the nuclear partial transitions in the charged pion photoproduction

R. A. Eramzhyan
Institute of Nuclear Research, U.S.S.R. Academy of Sciences, Moscow, U.S.S.R.

M. Gmitro
Institute of Nuclear Physics, Czechoslovak Academy of Sciences, CS 250 68 Řež, Czechoslovakia and Laboratory of Theoretical Physics, Joint Institute for Nuclear Research, Dubna, SU 101 000 Moscow, U.S.S.R.

S. S. Kamalov
Laboratory of Theoretical Physics, Joint Institute for Nuclear Research, Dubna, SU 101 000 Moscow, U.S.S.R.
(Received 14 September 1989)

Distorted-wave impulse approximation formalism in momentum space including the averaging over nucleon Fermi motion is presented for the case of nuclear pion photoproduction. Representative examples of the partial transitions on the ^{10}B, ^{12}C, ^{13}C, ^{14}N, and ^{15}N nuclei at several photon energies are compared with the data and discussed. This has enabled us to focus clearly on the successes and limitations in the present understanding of the nuclear photoproduction field.

I. INTRODUCTION

The experimental data of good quality for the pion photoproduction off light nuclei (from ^{3}He up to the oxygen isotopes) that have appeared in the last five years[1–4] strongly stimulated interest in the many-sided physics of this process. Specifically, one expects that the reaction with a well-defined nuclear final (bound) state, being free of the uncertainties of the nuclear continuum calculations, may provide a way to understanding the photoproduction mechanism.

Comparing with the data the results of the recent calculations one can see that several theoretical groups have met similar serious difficulties (e.g., strong and systematic underestimation of the differential cross sections for the ^{14}N(γ,π^+) ^{14}C reaction at $E_\gamma \gtrsim 250$ MeV) in spite of differences in the theoretical tools used such as the elementary photoproduction amplitude, treatment of the Δ_{33} isobar, pion distortion, etc. It seems to us that it is important to summarize for typical examples the points of agreement, and, maybe even more important, the points where all calculations disagree with the experimental data. We assume that such an analysis should become a starting point for the forthcoming search of the new physics still missing in our attempts to understand the $(\gamma,\pi^\pm)$ reactions.

To make our position clear, we should indeed present some details of our calculations. We work in the momentum representation.[5–9] In this approach it is computationally easier to control several features of the calculation, such as the full momentum dependence and off-shell continuation of the elementary photoproduction amplitude, the nucleon Fermi motion, etc. Our own early formulation[5] of distorted-wave impulse approximation (DWIA) in the momentum space has received important extensions. In our original version[5] we have treated the Fermi motion in the factorization approximation: instead of averaging over the nucleonic motion we have used the effective values of the nucleon momenta. In the present paper it is shown that the factorization is indeed an excellent approximation valid in many cases with an accuracy better than 1–2 %. There are, however, examples, where the genuine averaging cannot be avoided.

The important pion distortion effects are now incorporated via the momentum-space pion-nucleus optical potential developed in Refs. 10 and 11. There the microscopic first-order potential has been supplemented by a phenomenological term depending on the nuclear density squared. Such a potential is universal with respect to the atomic mass number $4 \leq A \leq 40$ and with respect to the pion charge.

Finally we wish to mention that the K-matrix approximation used in Ref. 5 is now avoided and the nuclear photoproduction amplitude is constructed with the off-mass-shell extrapolation included.

In Sec. II we present the formalism of our calculation. Section III contains an analysis of the representative examples of the partial $(\gamma,\pi^\pm)$ transitions in the p-shell nuclei. Conclusions and an outlook of the future work are given in Sec. IV.

II. DISTORTED-WAVE IMPULSE APPROXIMATION IN THE MOMENTUM SPACE

A. Effects of the pion-nucleus interaction

The general momentum-space formulation of the nuclear pion photoproduction as given in Ref. 5 allows us to take into account not only the single-particle photoproduction mechanism but also via channel coupling the multiparticle effects due to the two-step processes such as the virtual excitation and charge-exchange scattering.

Here we shall limit ourselves to a simpler version of the theory. The DWIA is constructed with the assumption

that the dominant distortion effects are due to the coherent scattering of the pion in the spherically symmetric part of the pion-nuclear optical potential ("coherent approximation").

We shall use the version of DWIA based on the Kerman-McManus-Thaler (KMT, Ref. 12) formulation of the multiple-scattering theory. The pion photoproduction matrix $T_{\pi\gamma}$ is

$$T^{fi}_{\pi\gamma}(\mathbf{q}_0,\mathbf{k}\lambda)=U^{fi}_{\pi\gamma}(\mathbf{q}_0,\mathbf{k}\lambda) + \int \frac{d^3q}{(2\pi)^3}\frac{T'(\mathbf{q},\mathbf{q}_0)U^{fi}_{\pi\gamma}(\mathbf{q},\mathbf{k}\lambda)}{\mathcal{E}_f(q_0)-\mathcal{E}_f(q)+i\epsilon}\ , \quad (1)$$

where $U^{fi}_{\pi\gamma}$ is the plane-wave photoproduction amplitude and $\mathcal{E}_f(q)=E_\pi(q)+E^f_A(q)$ is the total energy of the pion-nucleus system. As it is usual in KMT, we have introduced an auxiliary matrix T', which is connected with the true scattering matrix T via the relation

$$T'(\mathbf{q},\mathbf{q}_0)=\frac{A-1}{A}T(\mathbf{q},\mathbf{q}_0)\ . \quad (2)$$

The factor $(A-1)/A$ eliminates double counting of the pion-nucleon interaction acts included in the matrix $U^{fi}_{\pi\gamma}$. The T' matrix is in practice constructed as a solution of the Lippmann-Schwinger equation

$$T'(\mathbf{q},\mathbf{q}_0)=U_{\rm opt}(\mathbf{q},\mathbf{q}_0)+\int \frac{d^3q'}{(2\pi)^3}\frac{U_{\rm opt}(\mathbf{q},\mathbf{q}')T'(\mathbf{q}',\mathbf{q}_0)}{\mathcal{E}(q_0)-\mathcal{E}(q')+i\epsilon}\ . \quad (3)$$

The method of solution and the construction of the optical potential

$$U_{\rm opt}(\mathbf{q},\mathbf{q}_0)=U^{(1)}_{\rm opt}(\mathbf{q},\mathbf{q}_0)+U^{(2)}_{\rm opt}(\mathbf{q},\mathbf{q}_0;B_0,C_0) + V_{\rm Coul}(\mathbf{q}-\mathbf{q}_0;R) \quad (4)$$

are described in Ref. 11. The potential $U^{(1)}_{\rm opt}$ is microscopic and corresponds to the free pion-nucleon t matrix. The potential $U^{(2)}_{\rm opt}$ is proportional via phenomenological parameters B_0 and C_0 to the Fourier transform of the nuclear density squared. In Ref. 11 it has been demonstrated that universal (though energy-dependent) parameters B_0 and C_0 can be found such that they allow us to reproduce, with very good accuracy, all available total and elastic (differential and integral) cross sections for the $\pi^\pm$ scattering off light ($4\le A\le 40$) nuclei. The Coulomb interaction in the momentum space is treated as suggested by Vincent and Phatak;[13] in Ref. 13 one can also find the construction of the potential $V_{\rm Coul}$.

B. Nuclear photoproduction amplitude

In the basic photoproduction amplitude $U^{fi}_{\pi\gamma}$ that enters into Eq. (1) one disregards the distortion of the pionic waves. The amplitude $U^{fi}_{\pi\gamma}$ can be expanded over the single-nucleon states $\alpha\equiv(nlj)$ as

$$U^{fi}_{\pi\gamma}(\mathbf{q},\mathbf{k}\lambda)=\sum_{\alpha\alpha'}\langle f|c^+_{\alpha'}c_\alpha|i\rangle\langle \mathbf{q},\alpha'|\hat{t}_{\pi\gamma}|\alpha,\mathbf{k}\lambda\rangle\ , \quad (5)$$

where $|i\rangle$ ($|f\rangle$) is the nuclear initial (final) state, $\mathbf{q}$ is the pion momentum and $\mathbf{k}$ (λ) is the photon momentum (polarization). The matrix element of the pion photoproduction operator is

$$\langle \mathbf{q},\alpha'|\hat{t}_{\pi\gamma}|\alpha,\mathbf{k}\lambda\rangle=\int d^3p\ \phi^*_{\alpha'}(\mathbf{p}')\hat{t}_{\pi\gamma}(\mathbf{q},\mathbf{k}\lambda,\mathbf{p})\phi_\alpha(\mathbf{p})\ , \quad (6)$$

where $\mathbf{p}(\mathbf{p}')$ is the nucleon momentum in the initial (final) state. The spin-isospin structure of $\hat{t}_{\pi\gamma}$ is written in terms of cyclic components of the Pauli matrices σ and τ as

$$\hat{t}_{\pi\gamma}(\mathbf{q},\mathbf{k}\lambda,\mathbf{p})=(G_1\sigma_\lambda+\lambda G_2\sigma_0+G_3\sigma_{-\lambda}+G_4)\tau^\pm\ , \quad (7)$$

where

$$\tau^\pm=\mp(\tau_x\pm i\tau_y)/2=\tau_{\pm1}/\sqrt{2}\ .$$

The bound-nucleon wave function ϕ_α in the momentum space is

$$\phi_\alpha(\mathbf{p})=\sum_{m_s m_l}\begin{bmatrix} l & \frac{1}{2} & j \\ m_l & m_s & m\end{bmatrix}R_{nl}(\mathbf{p})Y_{lm_l}(\hat{\mathbf{p}})\chi_{m_s}\xi_{m_\tau}\ , \quad (8)$$

where $[\cdots]$ is the Clebsch-Gordan coefficient and χ_{m_s} (ξ_{m_τ}) stands for the nucleon spin (isospin) wave function. The other notation should be self-explanatory. The coefficients $G_\beta(1\le\beta\le4)$ define the specific features of the elementary $N(\gamma,\pi)N'$ amplitude.

Collecting together formulas (5)–(8) one can see that the decomposition

$$U^{fi}_{\pi\gamma}(\mathbf{q},\mathbf{k}\lambda)=(\hat{J}_f\hat{T}_f)^{-1}\sum_J\begin{bmatrix} J_i & J & J_f\\ M_i & M & M_f\end{bmatrix}\begin{bmatrix} T_i & 1 & T_f\\ N_i & N & N_f\end{bmatrix} \times U_{JM}f_{\rm c.m.}(\mathbf{q}-\mathbf{k}) \quad (9)$$

defines new amplitudes

$$U_{JM}=\sqrt{6}\hat{J}\sum_{nln'l'L}\left\{\sum_{\beta=1}^{3}\begin{bmatrix} L & 1 & J\\ M_L & \nu_\beta & M\end{bmatrix}\psi^{(n'l'nl)}_{J(L1),1}I^\beta_{LM_L}(n'l',nl)+\delta_{LJ}\delta_{M_LM}\psi^{(n'l'nl)}_{J(LO),1}I^4_{LM_L}(n'l',nl)\right\}\ , \quad (10)$$

where $\hat{J}=\sqrt{2J+1}$, $\nu_1=\lambda$, $\nu_2=0$, $\nu_3=-\lambda$, and $f_{\rm c.m.}(Q)=\exp(\frac{1}{4}Q^2b^2/A)$,

$$I^\beta_{LM_L}(n'l',nl)=(-)^{l+M_L}\int d^3p\ R_{n'l'}(\mathbf{p}')G_\beta(\mathbf{q},\mathbf{k}\lambda,\mathbf{p})R_{nl}(\mathbf{p})[Y_l(\hat{\mathbf{p}})\otimes Y_{l'}(\hat{\mathbf{p}}')]_{L,-M_L}\ . \quad (11)$$

The nuclear structure information is fully contained in the coefficients $\psi^{(n'l'nl)}_{J(LS),T}$, which are easily connected with the spin- and isospin-reduced matrix elements as

$$\psi^{(n'l'nl)}_{J(LS),T}=\sum_{j'j}\hat{S}\hat{L}\,\hat{j}'\hat{j}\begin{Bmatrix}\frac{1}{2} & \frac{1}{2} & S\\ j' & j & J\\ l' & l & L\end{Bmatrix}\psi_{JT}(\alpha',\alpha)\ , \tag{12}$$

where[6]

$$\psi_{JT}(\alpha',\alpha)=(\hat{J}\hat{T})^{-1}\langle J_f T_f|||[c^{+}_{\alpha'}\otimes\tilde{c}_{\alpha}]_{JT}|||J_i T_i\rangle\ .$$

All the results presented in this paper were obtained with the Blomqvist-Laget (BL) photoproduction amplitude.[14] Being constructed in an arbitrary frame of reference this amplitude is very well suited for the nuclear photoproduction calculations: the otherwise cumbersome transformation between the pion-nucleon and pion-nucleus center-of-mass systems is fully avoided. One should note that the BL amplitude[14] that we use is only partly unitarized. Namely, the most important Δ-isobar component of the amplitude is unitary by construction, at the same time the corresponding Born terms are left real. Criticism of this point has appeared in the literature, see, e.g., Ref. 9 and the references therein. The corresponding correction term

$$\sum_J[\exp(i\delta_J)-1]t^J_B\ ,$$

where t^J_B are the nonresonance amplitudes for multipoles J, is, however, small for the transitions dominated by the Kroll-Ruderman term since there even the dominant phase shift $\delta_0<10^\circ$ for $E^L_\gamma<300$ MeV. The opposite is, indeed, true for the partial transition $^{14}\mathrm{N}\rightarrow{}^{14}\mathrm{C}_{\mathrm{g.s.}}$ considered in Ref. 9: the Kroll-Ruderman term is heavily suppressed there and the importance of the correction terms grows. With this reservation we consider the partly unitarized BL amplitude[14] as an acceptable approximation. The explicit expressions of $G_\beta(1\le\beta\le4)$ for this amplitude are given in Appendix A.

C. Partial wave decomposition

For the numerical work we shall introduce the amplitudes $F_{\pi\gamma}$, $V_{\pi\gamma}$, and F', which are connected with the matrices $T_{\pi\gamma}$, $U_{\pi\gamma}$, and T' via the relations

$$F^{fi}_{\pi\gamma}(\mathbf{q}_0,\mathbf{k}\lambda)=-\frac{1}{2\pi}\sqrt{\mathcal{M}_i(k)\mathcal{M}_f(q_0)}\,T^{fi}_{\pi\gamma}(\mathbf{q}_0,\mathbf{k}\lambda)\ , \tag{13}$$

$$V^{fi}_{\pi\gamma}(\mathbf{q},\mathbf{k}\lambda)=-\frac{1}{2\pi}\sqrt{\mathcal{M}_i(k)\mathcal{M}_f(q)}\,\mathcal{V}^{fi}_{\pi\gamma}(\mathbf{q},\mathbf{k}\lambda)\ , \tag{14}$$

$$F'(\mathbf{q},\mathbf{q}_0)=-\frac{1}{2\pi}\sqrt{\mathcal{M}_f(q)\mathcal{M}_f(q_0)}\,T'(\mathbf{q},\mathbf{q}_0)\ , \tag{15}$$

where the relativistic reduced mass

$$\mathcal{M}_i(k)=kE^i_A(k)/\mathcal{E}_i(k)$$

$$[\mathcal{M}_f(q)=E_\pi(q)E^f_A(q)/\mathcal{E}_f(q)]$$

of the γ-nucleus [π-nucleus] system has been introduced. The pion energy is

$$E_\pi(q)=(m^2_\pi+\mathbf{q}^2)^{1/2}\ ,$$

and the energy of the nuclear initial (final) state is

$$E^{i(f)}_A=(M^{i(f)2}_A+\mathbf{q}^2)^{1/2}$$

with $M^{i(f)}_A$ for the nucleus rest mass.

We shall work with the partial pion-nucleus amplitudes F'_{L_π} defined by the decomposition

$$F'(\mathbf{q},\mathbf{q}_0)=4\pi\sum_{L_\pi M_\pi}\mathcal{F}'_{L_\pi}(q,q_0)Y^*_{L_\pi M_\pi}(\hat{\mathbf{q}}_0)Y_{L_\pi M_\pi}(\hat{\mathbf{q}})\ . \tag{16}$$

The on-mass-shell pion-scattering amplitude $\mathcal{F}'_{L_\pi}(q_0,q_0)$ can be connected with the pion-nucleus scattering phase shifts δ_{L_π} as

$$\mathcal{F}'_{L_\pi}(q_0,q_0)=\frac{1}{2iq_0}\frac{A-1}{A}(e^{2i\delta_{L_\pi}}-1)\ . \tag{17}$$

Taking the z axis of the coordinate system along the direction of the vector $\mathbf{k}$ we can write for the photoproduction amplitude $F^{fi}_{\pi\gamma}$ the decomposition

$$F^{fi}_{\pi\gamma}(\mathbf{q}_0,\mathbf{k}\lambda)=\sum_{L_\pi M_\pi}\mathcal{F}^{fi}_{L_\pi}(q_0,k\lambda)Y^*_{L_\pi M_\pi}(\hat{\mathbf{q}}_0)\ , \tag{18}$$

where $\mathcal{F}^{fi}_{L_\pi}$ is the photoproduction partial amplitude. An expansion of $V^{fi}_{\pi\gamma}$ fully analogous to Eq. (18) defines the plane-wave photoproduction partial amplitude $\mathcal{V}^{fi}_{L_\pi}(q,k\lambda)$. By substituting the three expansions into Eq. (1) one finds

$$\mathcal{F}^{fi}_{L_\pi}(q_0,k\lambda)=\mathcal{V}^{fi}_{L_\pi}(q_0,k\lambda)-\frac{1}{\pi}\int_0^\infty\frac{q^2dq}{\mathcal{M}_f(q)}\frac{\mathcal{F}'_{L_\pi}(q,q_0)\mathcal{V}^{fi}_{L_\pi}(q,k\lambda)}{\mathcal{E}_f(q_0)-\mathcal{E}_f(q)+i\epsilon}\ . \tag{19}$$

The amplitude $\mathcal{V}^{fi}_{L_\pi}$ is obtained from Eq. (14) as

$$\mathcal{V}^{fi}_{L_\pi}(q,k\lambda)=\int d\Omega_{\mathbf{q}}Y_{L_\pi M_\pi}(\hat{\mathbf{q}})V^{fi}_{\pi\gamma}(\mathbf{q},\mathbf{k}\lambda)=-\delta_{M_f+M_\pi,M_i+\lambda}\left[\frac{\mathcal{M}_i(k)\mathcal{M}_f(q)}{2\pi}\right]^{1/2}\int_{-1}^{1}dx\,P_{L_\pi M_\pi}(x)U^{fi}_{\pi\gamma}(q,x,\varphi_\pi=0,k\lambda)\ , \tag{20}$$

where $x=\cos\theta_\pi$ is an argument of the adjoint Legendre polynomial $P_{LM}(x)$. The x integration in Eq. (20) is performed numerically by using the Gauss-Legendre quadrature. The treatment of the singularity that appears in Eq. (19) is described in Appendix B.

Finally, for the photoproduction differential cross section we have

$$\frac{d\sigma_{fi}}{d\Omega}=\frac{q_0}{2k}\frac{1}{2J_i+1}\sum_{M_iM_f\lambda}\left|\sum_{L_\pi}C_{L_\pi}(q_0,R)\mathcal{F}^{fi}_{L_\pi}(q_0,k\lambda)Y^*_{L_\pi M_\pi}(\hat{\mathbf{q}}_0)\right|^2 , \tag{21}$$

where $M_\pi=M_i+\lambda-M_f$. The Coulomb factor $C_{L_\pi}(q_0,R)$ is obtained such that it assures the smooth matching at the point $r=R$ of the calculated (according to the procedure by Vincent and Phatak[13]) pionic wave function with the known Coulomb function that describes the pion motion in the asymptotic region. It should be noted that the factor $C_{L_\pi}(q_0,R)$ indeed also guarantees the correct threshold form of the differential cross section as obtained for the case of two (short-range plus long-range) potentials, e.g., in the monograph by Taylor.[15] In particular, for the s-wave component one can write

$$C_0(q_0,R)\underset{q\to 0}{\to}\frac{2\pi\kappa}{e^{2\pi\kappa}-1} , \tag{22}$$

where κ is the Sommerfeld parameter.

D. Averaging the nucleonic Fermi motion

In Eq. (11) we have reached the computationally most difficult point: after inserting Eq. (11) into Eq. (1) we face the six-dimensional integration $d^3q\,d^3p$. Frequently, in the analysis of purely nucleonic reactions, such integrals are approximated by the expansion

$$t(\mathbf{p})=t(0)+(\partial t/\partial\mathbf{p})|_{\mathbf{p}=0}\cdot\mathbf{p}+O(\mathbf{p}^2/m_N^2)$$

with the subsequent substitution $\mathbf{p}\to-i\nabla_r$, where the operator ∇_r acts on the wave function of the initial nucleus. This is impractical here since the photoproduction operator $\hat{t}_{\pi\gamma}$ as a function of $\mathbf{p}$ has a resonance character. This is due to the Δ-isobar contribution to $\hat{t}_{\pi\gamma}$ of the form $(W^2-M_\Delta^2+iM_\Delta\Gamma)^{-1}$, where

$$W^2=W_f^2\equiv[E_\pi(\mathbf{q})+E_N(\mathbf{p}')]^2-(\mathbf{q}+\mathbf{p}')^2 . \tag{23}$$

Earlier, in Ref. 5, for example, we have treated the nucleonic Fermi motion approximately. The method ("factorization approximation") suggested in Ref. 16 consists in the substitution

$$\mathbf{p}\to\mathbf{p}_{\text{eff}}=-\frac{\mathbf{k}}{A}-\frac{A-1}{2A}(\mathbf{k}-\mathbf{q}) \tag{24}$$

and allows an evaluation of $I^\beta_{LM_L}$ in the form $(1\le\beta\le4)$

$$I^\beta_{LM_L}(n'l',nl)\approx\sqrt{4\pi}\frac{\hat{l}\hat{l}'}{\hat{L}}Y^*_{LM_L}(\hat{\mathbf{Q}})i^L\begin{bmatrix}l & l' & L\\ 0 & 0 & 0\end{bmatrix}\times G_\beta(q,k\lambda,\mathbf{p}_{\text{eff}})\times\int_0^\infty R_{n'l'}(r)j_L(Qr)R_{nl}(r)r^2dr , \tag{25}$$

where $\mathbf{Q}=\mathbf{k}-\mathbf{q}$ is the transferred momentum and $j_L(Qr)$ is the spherical Bessel function. The error of the factorization approximation has been estimated[17] as being of the order $(m_\pi/m_N)^2$, where $m_\pi(m_N)$ is the pion (nucleon) mass.

In this paper we shall display results for the nuclear pion photoproduction cross sections calculated by numerical integration of (11) performed without further physical approximations and compare them, where appropriate, with those obtained via the factorization approximation. Details of our numerical procedure are given in Appendix C.

E. Comparison of the present method with other pion photoproduction calculations

Most traditionally[18] the DWIA calculations are performed in the coordinate space. The pionic plane-wave implicitly present in our Eq. (6) is there substituted by an outgoing distorted wave $\varphi^{(-)}_{\mathbf{q}_0}(\mathbf{r})$ and instead of Eq. (6) one writes

$$\langle\mathbf{q}_0,\alpha'|\hat{t}_{\pi\gamma}|\alpha,\mathbf{k}\lambda\rangle=\int d^3r\,\phi^*_{\alpha'}(\mathbf{r})\varphi^{(-)*}_{\mathbf{q}_0}(\mathbf{r})\hat{t}(\mathbf{q},\mathbf{k}\lambda,\mathbf{p})e^{i\mathbf{k}\cdot\mathbf{r}}\phi_\alpha(\mathbf{r}) . \tag{26}$$

The operators $\mathbf{q}=i\nabla_\pi$ and $\mathbf{p}=-i\nabla_\mathbf{r}$ act on the pionic function $\varphi^{(-)}_{\mathbf{q}_0}$ and the initial nucleon wave function, respectively. Technically, an ingoing solution $\varphi^{(+)}_{\mathbf{q}_0}(\mathbf{r})$ is usually constructed by solving the Klein-Gordon equation with some phenomenological optical potential and then the relation

$$\varphi^{(-)*}_{\mathbf{q}_0}(\mathbf{r})=\varphi^{(+)}_{-\mathbf{q}_0}(\mathbf{r}) \tag{27}$$

is used. The difficulties of such an approach are well known: the inclusion of the nucleonic Fermi motion is rather problematic, and, maybe even more important, the momentum dependence of the $\hat{t}_{\pi\gamma}$ matrix appearing, e.g., in the form $[(k-q)^2+m_\pi^2]^{-1}$, is difficult to treat properly.

To avoid the mentioned problems, Tiator and Wright[6] have calculated the matrix element (26) in the momentum space as

$$\langle\mathbf{q}_0,\alpha'|\hat{t}_{\pi\gamma}|\alpha,\mathbf{k}\lambda\rangle=\int d^3q\,d^3p\,\phi^*_{\alpha'}(\mathbf{p}')\varphi^{(-)*}(\mathbf{q},\mathbf{q}_0)\hat{t}_{\pi\gamma}(\mathbf{q},\mathbf{k}\lambda,\mathbf{p})\phi_\alpha(\mathbf{p}) , \tag{28}$$

where $\varphi^{(-)}(\mathbf{q},\mathbf{q}_0)$ is the Fourier transform of the function $\varphi^{(-)}_{\mathbf{q}_0}(\mathbf{r})$. Instead of our Eq. (27) one writes

$$\varphi^{(-)*}(\mathbf{q},\mathbf{q}_0)=\varphi^{(+)}(\mathbf{q},\mathbf{q}_0) . \tag{29}$$

Now it is easy to see the connection of the DWIA defined in Eq. (28) with the method we described. Trivially, for the plane wave solution $\varphi^{(+)}(\mathbf{q},\mathbf{q}_0)\to\delta(\mathbf{q}-\mathbf{q}_0)$,

Eq. (28) becomes Eq. (16). For the distorted waves represented as

$$\varphi^{(+)}(\mathbf{q},\mathbf{q}_0)=\delta(\mathbf{q}-\mathbf{q}_0)+\frac{T(\mathbf{q},\mathbf{q}_0)}{(2\pi)^3[\mathcal{E}(q_0)-\mathcal{E}(q)+i\epsilon]} \tag{30}$$

one observes that an expression similar to Eq. (1) is obtained from Eq. (28). They differ, however, by the factor $(A-1)/A$, which eliminates certain double countings as discussed in connection with Eq. (1).

Another, numerically more important difference between the two approaches is due to a different choice of kinematic quantities. In the present calculation, we have taken the pion energy as

$$E_\pi=E_\pi(\mathbf{q})\equiv(m_\pi^2+\mathbf{q}^2)^{1/2} \tag{31}$$

and in the Δ-resonance propagator the total energy W of the π-nucleus system is chosen as $W=W_f$ [see Eq. (23)]. At the same time Tiator and Wright[6] use

$$E_\pi^{\mathrm{TW}}=(m_\pi^2+\mathbf{q}_0^2)^{1/2} \tag{32}$$

where $\mathbf{q}_0$ is the on-shell (asymptotic) pion momentum. Also they take

$$W^{\mathrm{TW}}=W_i\equiv\{[E_\gamma+E_N(\mathbf{p})]^2-(\mathbf{k}+\mathbf{p})^2\}^{1/2} \tag{33}$$

in the Δ-isobar propagator. As for the comparison of the two models, we wish to quote the detailed analysis of the neutral pion photoproduction by Chumbalov and Kamalov.[19] They point towards an important priority of the choice $W=W_f(\mathbf{q},\mathbf{p})$ and $E_\pi=(m_\pi^2+\mathbf{q}^2)^{1/2}$, where the pion energy is not constant but rather it is systematically expressed via the integration variable $\mathbf{q}$, the local pion momentum.

Finally, we would like to mention that the Coulomb interaction ignored in Ref. 6 finds an appropriate treatment in our calculation, as explained in Sec. II C. From the results it is obvious that, though unimportant at the resonance energies, the Coulomb interaction cannot be neglected in the near threshold pion photoproduction.

III. RESULTS

A. $^{10}\mathrm{B}(\gamma,\pi^+)\,^{10}\mathrm{Be}_{\mathrm{g.s.}}$

Here we have a $3^+0\to0^+1(J_iT_i\to J_fT_f)$ transition, this is a $M3$ multipole with the dominant $[\sigma\otimes Y_2]_3$ operator. Such a clean structure leads to the assumption that

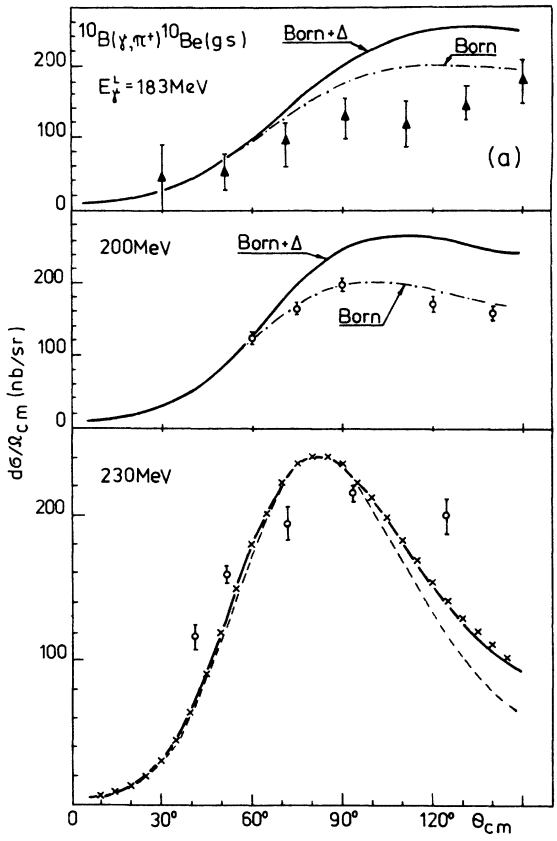

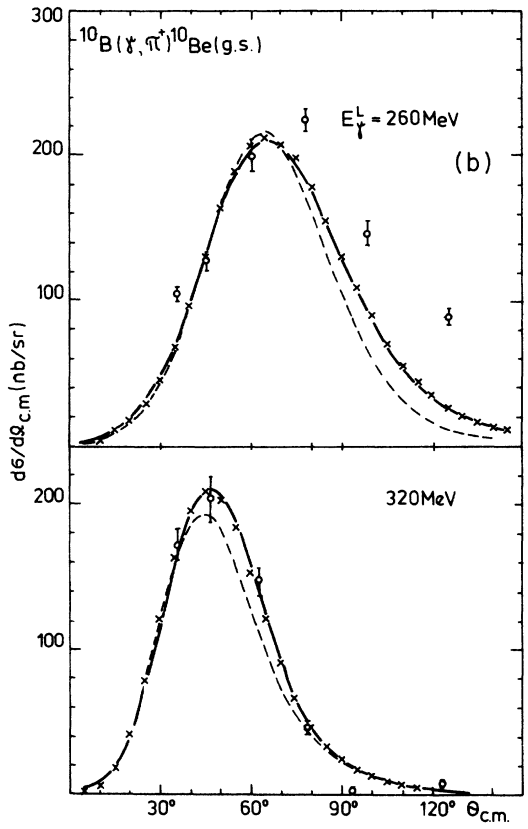

FIG. 1. DWIA pion angular distributions for the $^{10}\mathrm{B}(3^+0)\,(\gamma,\pi^+)^{10}\mathrm{Be}(0^+1)$ reaction calculated with the Cohen and Kurath (Ref. 20) transition density at (a) $E_\gamma^{\mathrm{lab}}=180$, 200, and 230 MeV; and (b) 260 and 320 MeV using the complete BL amplitude (Ref. 14). Nucleonic Fermi motion is numerically averaged (full line), treated within the factorization approximation (lines marked with ×'s, see the text), and disregarded (dashed line). Dash-dotted line corresponds to the results obtained without the Δ-isobar component of the BL amplitude. The experimental data are from Ref. 4 (triangles) and Ref. 21 (open circles).

the corresponding electron-scattering data may provide us with the necessary nuclear structure information in a broad interval of the transferred momenta. The high multipolarity of this transition suggests that the nuclear interior should not strongly influence the results. In other words the behavior of the pionic wave function inside the nucleus should not be important for our purpose.

The nuclear transversal density has been obtained from the Cohen-Kurath wave functions,[20] which in this case describe the experimental form factor correctly. The density is determined by the coefficient [see Eq. (12)] $\psi_{3(21),T=1}=0.582$ and the oscillator parameter is $b=1.66$ F, both values are taken from Ref. 18.

The calculated photoproduction differential cross sections are displayed in Fig. 1. There are three types of calculations: (i) nucleonic Fermi-motion disregarded, (ii) factorization approximation [Eq. (24)], and (iii) averaging over the nucleonic Fermi motion performed numerically.

Fully disregarding the Fermi motion ($\mathbf{p}=-\mathbf{k}/A$, $\mathbf{p}'=\mathbf{p}+\mathbf{k}-\mathbf{q}$) one obtains results considerably different from those of the full calculation, as in (iii). The disagreement grows with the pion energy. This is obviously connected with the growing role at higher energies of the Δ-resonance mechanism: the Δ-isobar propagator with its strong momentum dependence shows up in the Fermi averaging. On the other hand one can see that the factorization approximation (the curve marked with ×'s, to be compared with the solid lines) provides differential cross sections that differ at most by 1–2 % from those obtained by the numerical Fermi averaging.

Let us now compare the theoretical results with the data. For the pion energies above the (3,3) resonance the calculated differential cross section is in an agreement with the recent MIT data.[21] We miss, however, an understanding of the photoproduction mechanisms at lower energies: the experimental data at $E_\gamma \leq 200$ MeV clearly prefer the calculations with the Δ-resonance term omitted. A possible reason for it can be connected with some suppression of the Δ-resonance mechanism in the nuclear medium. Similar suppression effects can be seen in the calculations performed within the isobar-doorway model[22] and delta-hole model[23] for the coherent production of π^0 mesons. A final answer to this problem can possibly be found in a unified analysis (coupled channels) of the neutral and charged pion photoproduction.

Another possible explanation of the observed suppression of the $d\sigma/d\Omega$ at $E_\gamma \leq 200$ MeV could be connected with the pion-propagator modification in the t-channel exchange pion diagram, which is indeed specific for the charged pion photoproduction.[24]

As for the comparison with the results of other calculations we wish to comment that, intrinsically, our DWIA method requires the extrapolation of the elementary amplitude into the off-energy-shell region in the form $E_\pi=(m_\pi^2+\mathbf{q}^2)^{1/2}$ ($\mathbf{q}$ is the local pion momentum). With such a choice our results differ from those by Tiator[25] at most by 10% at $E_\gamma \gtrsim 260$ MeV, the difference being almost negligible (2–3 %) at lower energies. Taking the pion off-shell-energy extrapolation as $E_\pi=(m_\pi^2+\mathbf{q}_0^2)^{1/2}$ ($\mathbf{q}_0$ is the pion asymptotic momentum), which corresponds to Tiator and Wright's version of DWIA, we indeed found even a better agreement of the two theories: the difference between their and our result does not exceed 5% at $E_\gamma \leq 260$ MeV and 7% at $E_\gamma=320$ MeV. Such a nice coincidence of two rather different calculations shows that the $^{10}\mathrm{B}\rightarrow{}^{10}\mathrm{Be}_{\mathrm{g.s.}}$ photoproduction transition is rather insensitive to the construction of the transition operator and to the particular form of the pionic optical potential.

B. $^{12}\mathrm{C}(\gamma,\pi^+)^{12}\mathrm{B}_{\mathrm{g.s.}}$

In this partial transition one should consider simultaneously two nuclear transition densities, namely those with $L=0$ and $L=2$. Unlike the case of ^{10}B, here the magnetic-type form factor calculated with the Cohen-Kurath wave functions does not reproduce the experimentally observed second maximum of the form factor at $Q\approx 2$ F^{-1}, which is due to the interference of the $L=0$ and 2 components of the transition density. Dubach and Haxton[26] have suggested that the failure is connected with the absence of the $2\hbar\omega$ components in the Cohen-Kurath wave functions. To avoid the configuration mixing calculations in an extended space, Dubach and Hax-

TABLE I. Coefficients $\psi_{J(LS),T=1}$ [LS coupling, see Eq. (12)] and the values of the oscillator constant b used in the calculation of the reduced density matrix elements. Spin, parity, and isospin on the nuclear initial and final states are given in the second row. The final nucleus is always in its ground state.

				$^{13}\mathrm{C}\rightarrow{}^{13}\mathrm{N}$		$^{14}\mathrm{N}\rightarrow{}^{14}\mathrm{C}$			
			$^{12}\mathrm{C}\rightarrow{}^{12}\mathrm{B}$	$\frac{1}{2}^-\frac{1}{2}\rightarrow\frac{1}{2}^-\frac{1}{2}$		$1^+0\rightarrow 0^+1$			$^{15}\mathrm{N}\rightarrow{}^{15}\mathrm{O}$
J	L	S	$0^+0\rightarrow 1^+1$	TW	S	$H1$	$H2$	$HF2$	$\frac{1}{2}^-\frac{1}{2}\rightarrow\frac{1}{2}^-\frac{1}{2}$
0	0	0		0.577	0.578				0.577
0	1	1		0.390	−0.051				0.817
1	1	0	0.101	0.186	0.193	0.339	0.418	−0.180	−0.437
1	0	1	−0.258	−0.158	−0.159	−0.033	−0.042	0.0	0.179
1	1	1	−0.239	0.0	0.0	0.041	0.0	−0.009	0.0
1	2	1	0.016	0.343	0.585	0.435	0.395	−0.497	−0.799
b (F)			1.76	1.73	1.73	1.70	1.70	1.70	1.67
Reference			26	6	18(b)	33	33	33	30

ton[26] keep the form of the $M1$ transition density the same as it is obtained for the pure p-shell model and treat the coefficients that define the density as phenomenological parameters. Being obtained by a fit to the data the coefficients $\psi_{J(LS),T}$ are supposed to have absorbed the effects of the omitted $2\hbar\omega$ configurations. The density is denoted as DH here and the corresponding coefficients $\psi_{J(LS),T}$ are listed in Table I. Earlier we calculated the differential cross sections for the pion inelastic scattering using both the Cohen-Kurath and DH models. The calculation[27] shows a clear preference to the DH density.

The results of our DWIA pion photoproduction calculations performed with the DH density are shown in Fig. 2. Again the factorization approximation provides the photoproduction cross sections, which agree very well with those obtained via the full Fermi integration.

The calculated cross sections for the low pion energies at backward angles go substantially lower than the experimental results. This discrepancy should partly be connected with the large interference term of the $L=0$ and 2 components of the nuclear transition density. This means that the photoproduction cross sections are very sensitive to the details of the pion-nuclear optical potential.[27] Later we shall observe an almost identical situation for the $^{14}N \rightarrow {}^{14}C_{g.s.}$ transition.

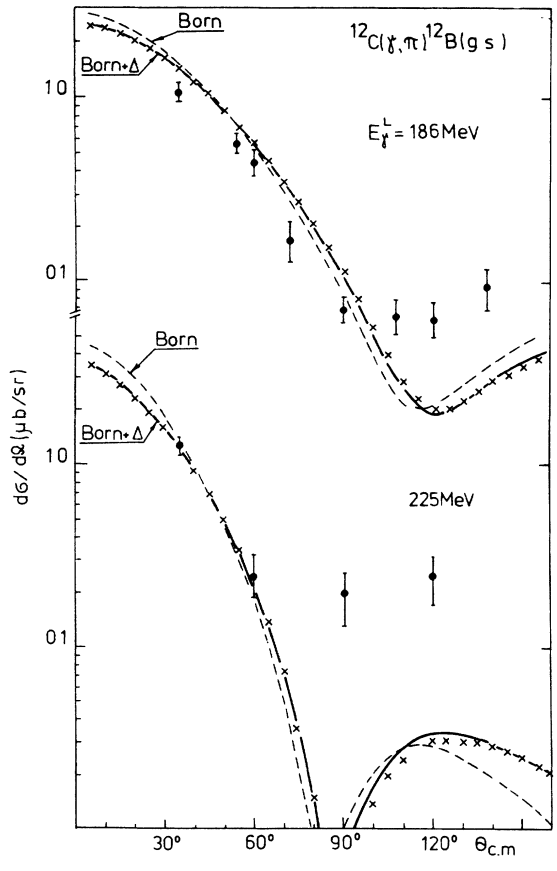

FIG. 2. DWIA pion angular distributions for the $^{12}C(0^+0)$ (γ,π^+) $^{12}B(1^+1)$ reaction calculated with the DH transition densities (Ref. 26). The full line (lines marked with ×'s) corresponds to the complete BL amplitude (Ref. 14) and numerical Fermi motion averaging (factorization approximation), dashed line is for BL amplitude without the Δ-isobar component. The experimental data are from Ref. 28 for $E_\gamma^{lab}=186$ MeV and Ref. 29 for $E_\gamma^{lab}=225$ MeV.

The assumption about the importance of the interference effects in $M1$-type transitions can be checked in the $1^+0 \rightarrow 0^+1$ transition in ^{6}Li. That $M1$ transition is indeed similar to the cases considered here ($A=12$ and 14 nuclei); however, it is almost insensitive to the interference phenomena just discussed. This is so since due to the specific properties of the ^{6}Li wave function, the $L=2$ component of the $M1$ density is very small in ^{6}Li. These relations have found a direct support in the calculation of the corresponding electromagnetic form factor and (γ,π^+) cross sections. If calculated with the p-shell model wave functions they agree reasonably well with their experimental counterparts.[27]

The role of the Δ-isobar term is at low energies of pions very similar to that observed for the $^{10}B \rightarrow {}^{10}Be_{g.s.}$ transition. Switching off the Δ-isobar term of the elementary photoproduction amplitude decreases the cross sections at larger ($\theta_\pi \geq 50°$) angles and increases them for the forward angles. Such a behavior is general for the magnetic-type transitions in the ^{10}B, ^{12,13}C, and ^{15}N targets that we have considered and is connected with the $\cos\theta_\pi$ dependence of the dominant contribution of the Δ-isobar term.

We have calculated the $^{12}C \rightarrow {}^{12}B_{g.s.}$ photoproduction cross section also at $E_\gamma=197$ MeV (not shown in Fig. 2), which can be compared with that obtained by Singham and Tabakin[18] who have used the same nuclear wave functions (DH density). The two theoretical curves differ by less than 10% for $\theta_\pi<90°$, the difference reaches about 30% at the extreme backward angles. This difference can be connected with the variation of the pion optical potentials used in the two calculations.

C. $^{13}C(\gamma,\pi^-)^{13}N_{g.s.}$ and $^{15}N(\gamma,\pi^-)^{15}O_{g.s.}$

It is convenient to discuss these two transitions together since in both cases we observe a combination of the magnetic-type $M1$ transition with the electric-type $E0$ transition. What is more important, the conventional shell-model wisdom suggests that the two transitions should show very similar features since in both cases the initial and final nuclear states are isobar analogs. This means that the net effect of the (γ,π^-) reaction consists only in "shaking up" the isospin variables. Actually the calculations corroborate such a picture: the $E0$ transition densities are practically the same in the two cases, and for the $M1$ densities one sees only minor difference connected with different weights of the $L=2$ component in the $A=13$ and 15 nuclei (see Table I). In view of this it is clear that the calculated photoproduction cross sections should appear very similar for the two target nuclei. At the same time the experimental cross sections show a qualitatively different behavior.

In the calculations we have used the semiphenomenological transition densities taken from Refs. 6, 18b, and 30. The $M1$ transition density has been constructed in the course of analysis of the electromagnetic form factor,

the static properties of the initial and final nucleus, and the beta decay rate. The TW density[6] is also constrained by the then available (γ,π) data. The $E0$ component is that of Cohen and Kurath.[20] The respective coefficients $\psi_{J(LS),T}$ are given in Table I.

The calculated differential cross sections are displayed in Fig. 3 and 4. Again, the factorization approximation appears to be fully valid and can be used for the quantitative discussion.

As for the comparison with the data one observes for $^{13}C(\gamma,\pi^-)$ a serious disagreement in the forward hemisphere ($\theta_\pi \lesssim 90°$). A possible explanation may again as in the case of the ^{10}B nucleus be connected with the need for suppression of the Δ-isobar term of the photoproduction amplitude. Actually after switching off the Δ term of the BL amplitude one obtains the cross section, which agrees nicely with the data.

The conclusion just drawn is, however, strongly connected with the choice of the underlying transition densities. The TW densities[6] used above has been obtained via a fitting procedure that is not free of criticism. Singham[18(b)] has pointed out that there is no nuclear wave function within the $1p$ shell that could possibly produce them.

Starting with the wave functions of $^{13}C_{g.s.}$ and $^{13}N_{g.s.}$ Singham[18(b)] has derived four sets of the transition densities free of the above criticism. We have repeated our calculation with his set I. In Table I the corresponding coefficients are given, and the dotted lines in Fig. 3 show the calculated (γ,π^-)-differential cross sections. The latter are in a qualitative agreement with the coordinate-space result shown in Ref. 18(b). We observe, however, a substantial disagreement with the data, especially for the backward angles. The difference between the two calculations is connected with the change of the weights of the $L=0$ and 2 components of the $M1$ densities derived in Ref. 6 and Ref. 18(b). A similar situation has already been observed in Ref. 27 for the $M1$ transition in ^{12}C.

Turning now to the case of the $^{15}N(\gamma,\pi^-)$ reaction one can see that the calculation underestimates the data at the forward angles roughly twice. Switching off the Δ-isobar contribution, which has helped in the previous examples, further deteriorates the comparison with the data for $\theta_\pi < 90°$. For the backward angles one does not see any serious discrepancy between theory and experiment in either of the two cases. Very similar results for these partial transitions have been obtained by Tiator *et al.*[30] They differ from those displayed here by less than ten per cent.

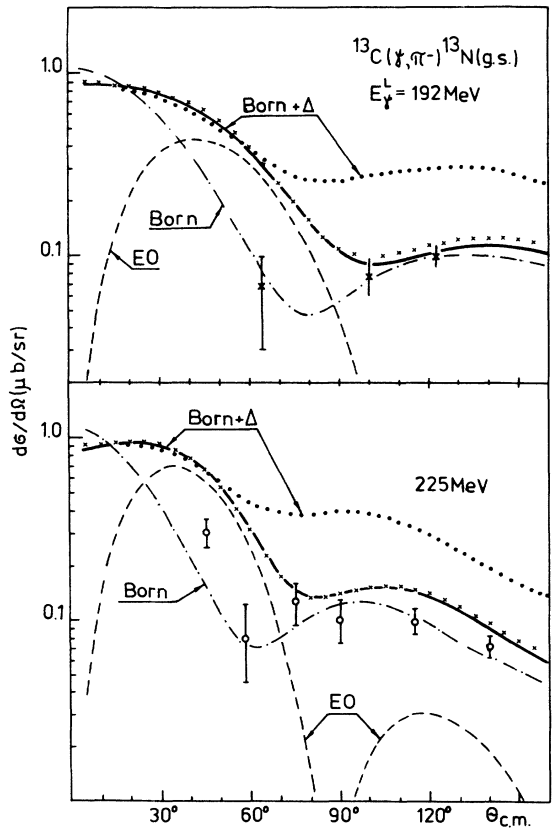

FIG. 3. DWIA pion angular distributions for the $^{13}C(\frac{1}{2}^-\frac{1}{2})$ (γ,π^-) $^{13}N(\frac{1}{2}^-\frac{1}{2})$ reaction calculated with the TW transition densities (Ref. 6). Meaning of the lines is the same as in Fig. 1. Dotted line corresponds to the transition density by Singham [Ref. 18(b)]. Dashed line is for the $E0$ contribution with the complete BL amplitude (Ref. 14). Data are from Ref. 31 for $E_\gamma^{lab}=192$ MeV and from Ref. 32 for $E_\gamma^{lab}=225$ MeV.

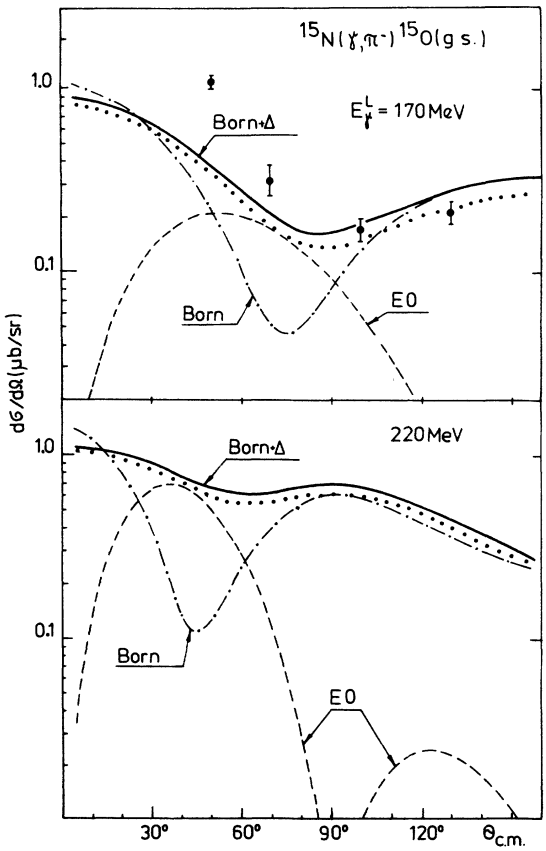

FIG. 4. The same as in Fig. 3 but for the $^{15}N(\frac{1}{2}^-\frac{1}{2})(\gamma,\pi^-)$ $^{15}O(\frac{1}{2}^-\frac{1}{2})$ reaction. Dotted line corresponds to the calculation with the Coulomb interaction disregarded. Data are from Ref. 30.

The analysis of the $^{13}C \rightarrow {}^{13}N$ and $^{15}N \rightarrow {}^{15}O$ photoproduction transitions is strongly hindered by the absence of any independent check for the corresponding $E0$ transition densities, which cannot be separated out from the electron scattering experiments and $L=0$ and 2 components in the $M1$ transition density. Additional independent information can, however, in principle be obtained from the experimental and theoretical analysis of the ^{13}C, $^{15}N(\pi^+,\pi^0)$ charge-exchange reaction at low energies and elastic pion scattering. In particular the polarization characteristics of these reactions may throw light on the $E0$-$M1$ interference effects.

Here we also wish to illustrate the role of the Coulomb interaction in the pion photoproduction calculations. As can be expected, the attractive Coulomb potential, e.g., in the $^{15}N(\gamma,\pi^-)$ reaction modifies rather strongly (c.f. a dotted line in Fig. 4) the photoproduction cross section at low energies and backward angles. With the growing energy and in the forward hemisphere the importance of the Coulomb interaction indeed drops.

D. $^{14}N(\gamma,\pi^+)^{14}C_{g.s.}$

The results are displayed in Fig. 5. There are three important contributions to this transition. The components $[\sigma \otimes Y_0]_1$ and $[\sigma \otimes Y_2]_1$ are large but interfere destructively. The third one connected with the operator $[Y_1 \otimes \nabla]_1$ does not contribute in the factorization approximation and provides a nonzero contribution only when complete Fermi-averaging is performed. This situation indeed explains the substantial difference between the results obtained within the factorization approximation and in the full calculation in this case.

The above mentioned strongly destructive interference of the dominant matrix elements in this transition actually explains its very specific behavior: the photoproduction cross sections are in this case strongly sensitive even to small variations of the corresponding wave functions. In such a situation one can hardly expect a quantitative agreement between theory and data; still we think that some qualitative features can be extracted from such a comparison.

In Fig. 5(a) we show the photoproduction cross sections for the low pion energies where the interference effects between $L=0$ and 2 components are particularly strong. Three versions of the nuclear transition densities are taken from Ref. 33. There an attempt has been made to deduce the transition density from the electron scattering experiments and static properties of the $A=14$ nuclei. The comparison of our calculated photoproduction cross sections at $E_\gamma = 173$ and 200 MeV with data shows that the $H1$ and especially the $H2$ version of the shell-

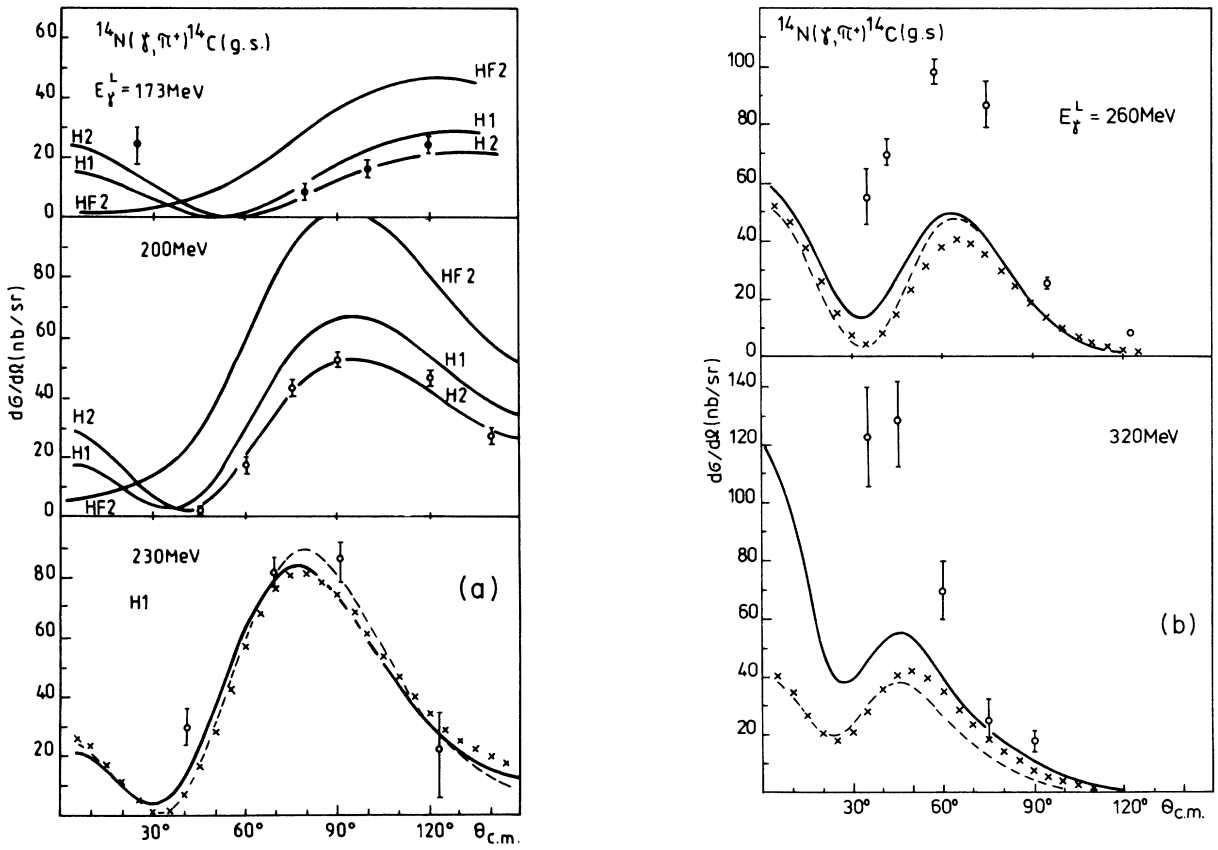

FIG. 5. The same as in Fig. 1 but for the $^{14}N(1^+0)$ (γ,π^+) $^{14}C(0^+1)$ reaction, and (a) $E_\gamma^{lab}=173$, 200, and 230 MeV, (b) $E_\gamma^{lab}=260$ and 320 MeV. The $H1$ nuclear transition density (Ref. 33) has been used if not stated otherwise. Data are from Ref. 4 (dots) and Refs. 2, 3, and 21 (open circles).

model density provides results close to the experiment. In their construction it has been assumed, that the well-known low value of the beta-decay rate in ^{14}C is due to the destructive combination of the one-body terms with the meson-exchange current contributions. The third density denoted as *HF*2 is constructed under the assumption that the Gamov-Teller operator ($L=0$) is fully switched off $\psi_{1(01),1}=0$. Such a density when used for the photoproduction calculations leads to the results that contradict the data.

If the low-energy data can be described at least with one nuclear transition density, the situation at the energies near the Δ_{33} resonance is fully different. Our calculations independently of the choice of the transition density underpredict the photoproduction data by a factor of 2 or more. Precisely the same tendency has been found in several earlier theoretical works. Most elaborated among them apparently is the calculation by Tiator *et al.*[8] Our calculated differential cross sections differ from their DWIA results by 20% at $E_\gamma=200$ MeV; the difference reaches, however, 80% at the higher energies of the incident photon. Being closer to the experimental values, the results of Ref. 8 nevertheless still underestimate strongly the high energy data. The reason for such a failure in all available calculations is not clear. Our calculations provide the photoproduction cross sections that are close to those obtained by Tiator *et al.* within the Δ-*h* model.[8] At $E_\gamma=230$ MeV the cross section in its maximum differs by less than 10% in the two calculations. Unfortunately, a detailed comparison is difficult to perform since the effects due to the Δ-propagator modification (in the elementary photoproduction amplitude) are in Ref. 8 obscured by the additional effects connected with the difference between the pionic wave calculated with the SMC (Ref. 34) optical potential and that pertaining to the Δ-*h* model. We expect that the last effect is the most important and the pion wave function obtained within the Δ-*h* model is close to ours.

As was discussed in Sec. II B, the transition $^{14}N\rightarrow{}^{14}C_{g.s.}$ may receive additional contributions if also the Born amplitude is properly unitarized.[9]

IV. CONCLUSIONS

In the present paper we have developed a new version of the pion-photoproduction DWIA in the momentum space. It differs from the traditional coordinate space methods since it allows a straightforward consideration of both the pion and nucleon nonlocalities in the photoproduction operator. Unlike the momentum-space DWIA of Refs. 6 and 7 our method is well suited for the simultaneous description of the pion scattering and photoproduction reactions. In addition, we describe both processes in the momentum space and this allows a fully consistent consideration of the corresponding nonlocalities.

Using as examples several photoproduction partial transitions in the *p*-shell nuclei we have seen that the factorization approximation of Eq. (24) can be used as a highly effective tool for calculating the $(\gamma,\pi^{\pm})$ cross sections. Being numerically extremely effective, it allows the estimates that differ in the majority of examples by less than 2–3 % from the complete calculation including integration over nucleon momenta. The approximation is effective and precise in all transitions dominated by the $\sigma\cdot\epsilon$ (Kroll-Rudermann) term, which is independent of the nucleonic coordinates. If the higher terms depending on the nucleon momenta become very important due to the suppression of the Kroll-Ruderman term (e.g., the $^{14}N_{g.s.}\rightarrow{}^{14}C_{g.s.}$ transition) the factorization approximation ceases to be useful and the complete machinery of the Fermi averaging must be utilized if one needs quantitatively correct results. These cases are, however, easy to separate from the very beginning.

Our analysis of several 1*p*-shell photoproduction transitions at different energies has shown that the difficulties already observed in earlier calculations[18] are general and most probably inherent in the DWIA method in its present formulations. Actually, one cannot achieve a consistent description of the data. Especially severe are problems at low photon energies, $E_\gamma\leq 200$ MeV. In two cases (the $^{10}B\rightarrow{}^{10}Be$ and $^{13}C\rightarrow{}^{13}N$ transitions) the agreement with data can be obtained by switching off the Δ-isobar term of the elementary photoproduction amplitude. It is tempting to speculate that this experience may suggest existence of some mechanism suppressing the role of the Δ isobar at low energies. The "model" does not help to account for the problems arising with the photoproduction transitions in ^{12}C and ^{15}N.

For higher photon energies, $E_\gamma>230$ MeV, which come close to the Δ-resonance region, we suffer from the lack of experimental data. The only examples studied experimentally for the *p*-shell nuclei, the cases of the ^{10}B and ^{14}N targets show a different behavior. The pion photoproduction on ^{10}B is at high photon energies correctly described within DWIA. At the same time the $^{14}N(\gamma,\pi^{+})$ reaction is notoriously known[8,9] to produce more serious problems for theory: the calculated (γ,π^{+}) cross sections at $E_\gamma\geq 260$ MeV systematically turn out much too low by a factor 2–3.

A further work should apparently go beyond the DWIA frame if a consistent picture of the charged pion photoproduction is to be developed. The most important effects to be studied now are, in our opinion, (i) modification of the Δ-isobar propagator, (ii) modification of the pion propagator in the nuclear medium, and (iii) inclusion of the two-step processes, namely, those connected with the pion charge-exchange reaction. The formalism described in the present paper is well suited for that task.

ACKNOWLEDGMENTS

We would like to thank Dr. R. Mach for fruitful collaboration on an early stage of this work and Dr. A. M. Bernstein and Dr. L. Tiator for very useful discussions on the subject.

APPENDIX A: UNITARIZED VERSION OF THE BLOMQVIST-LAGET AMPLITUDE

The photon polarization vectors ϵ_λ ($\lambda=\pm 1$) are defined by the unit vectors $\mathbf{e}_x$ and $\mathbf{e}_y$ as

$$\epsilon_\lambda = -\frac{\lambda}{\sqrt{2}}(\mathbf{e}_x + i\lambda \mathbf{e}_y) . \tag{A1}$$

To express the BL amplitude in form (7), we shall apply the formula

$$\mathbf{A}\cdot\mathbf{B} = \mathbf{A}\cdot\boldsymbol{\epsilon}_\lambda \mathbf{B}\cdot\boldsymbol{\epsilon}_\lambda^* + \mathbf{A}\cdot\boldsymbol{\epsilon}_\lambda^* \mathbf{B}\cdot\boldsymbol{\epsilon}_\lambda + \mathbf{A}\cdot\hat{\mathbf{k}}\mathbf{B}\cdot\hat{\mathbf{k}} \tag{A2}$$

valid for arbitrary vectors $\mathbf{A}$ and $\mathbf{B}$ if $\hat{\mathbf{k}} = \mathbf{e}_z$ is the unit vector along $\mathbf{k}$. Then, using the notation as in the paper by Singham and Tabakin[18] we can write the coefficients G_β as

$$G_\beta = G_\beta(\text{Born}) + G_\beta(\Delta), \quad \beta = 1,2,3,4 , \tag{A3}$$

where, for the $(\gamma,\pi^\pm)$ reaction

$$G_1(\text{Born}) = \frac{\sqrt{2}eg}{2m_N}\left[\mp 1 + \frac{m_N E_\pi}{E_x(p_x^0 + E_x)} - M^{(-)}\mathbf{q}\cdot\mathbf{k} \mp \frac{2\mathbf{q}\cdot\boldsymbol{\epsilon}_\lambda \mathbf{q}\cdot\boldsymbol{\epsilon}_\lambda^*}{(k-q)^2 - m_\pi^2} - \frac{\mathbf{p}_N\cdot\boldsymbol{\epsilon}_\lambda \mathbf{q}\cdot\boldsymbol{\epsilon}_\lambda^*}{E_x(p_x^0 - E_x)} \right] ,$$

$$G_2(\text{Born}) = \lambda\frac{\sqrt{2}eg}{2m_N}\left[M^{(-)}E_\gamma \mathbf{q}\cdot\boldsymbol{\epsilon}_\lambda \pm \frac{2\mathbf{q}\cdot\boldsymbol{\epsilon}_\lambda(E_\gamma - \mathbf{q}\cdot\hat{\mathbf{k}})}{(k-q)^2 - m_\pi^2} - \frac{\mathbf{p}_N\cdot\boldsymbol{\epsilon}_\lambda \mathbf{q}\cdot\hat{\mathbf{k}}}{E_x(p_x^0 - E_x)} \right] , \tag{A4}$$

$$G_3(\text{Born}) = \frac{\sqrt{2}eg}{2m_N}\left[\pm\frac{\mathbf{q}\cdot\boldsymbol{\epsilon}_\lambda \mathbf{q}\cdot\boldsymbol{\epsilon}_\lambda}{(k-q)^2 - m_\pi^2} + \frac{\mathbf{p}_N\cdot\boldsymbol{\epsilon}_\lambda \mathbf{q}\cdot\boldsymbol{\epsilon}_\lambda}{E_x(p_x^0 - E_x)} \right] ,$$

$$G_4(\text{Born}) = -\lambda\frac{\sqrt{2}eg}{2m_N} M^{(+)}E_\gamma \mathbf{q}\cdot\boldsymbol{\epsilon}_\lambda .$$

The factor $M^{(\pm)}$, again using the notation of Ref. 18 is

$$M^{(\pm)} = \frac{\mu_A}{2E_a(p_a^0 - E_a)} \pm \frac{\mu_B}{2E_b(p_b^0 - E_b)} . \tag{A5}$$

The Δ-isobar contributions are

$$\begin{aligned} G_1(\Delta) &= \tfrac{1}{3}R_\Delta(\mathbf{Q}_\Delta\cdot\mathbf{K}_\Delta - \mathbf{Q}_\Delta\cdot\boldsymbol{\epsilon}_\lambda \mathbf{K}_\Delta\cdot\boldsymbol{\epsilon}_\lambda^*) , \\ G_2(\Delta) &= -\tfrac{1}{3}\lambda R_\Delta \mathbf{Q}_\Delta\cdot\boldsymbol{\epsilon}_\lambda \mathbf{K}_\Delta\cdot\hat{\mathbf{k}} , \\ G_3(\Delta) &= \tfrac{1}{3}R_\Delta \mathbf{Q}_\Delta\cdot\boldsymbol{\epsilon}_\lambda \mathbf{K}_\Delta\cdot\boldsymbol{\epsilon}_\lambda , \\ G_4(\Delta) &= -\tfrac{2}{3}iR_\Delta \mathbf{Q}_\Delta\cdot\mathbf{K}_\Delta\times\boldsymbol{\epsilon}_\lambda , \end{aligned} \tag{A6}$$

where $\mathbf{Q}_\Delta = \mathbf{q} - E_\pi \mathbf{p}_a/M_\Delta$ and

$$\mathbf{K}_\Delta = \mathbf{k} - (M_\Delta - m_N)\mathbf{p}/m_N .$$

The quantity $R_\Delta(W)$ depends only on the total pion-nucleon energy W in their center-of-mass system. We have

$$R_\Delta(W) = C_\pi C_\gamma C_1 C_3 e^{i\psi_1}(W^2 - M_\Delta^2 + iM_\Delta\Gamma)^{-1} , \tag{A7}$$

where $C_\pi C_\gamma = \mp\frac{1}{3}\sqrt{2}$ for the $\pi^\pm$ photoproduction, and $M_\Delta = 1225$ MeV. The coupling constants are

$$C_1 = 0.34\sqrt{4\pi/137}\,\frac{M_\Delta + m_N}{m_{\pi^\pm}}, \quad C_3 = \frac{2.18}{m_{\pi^+}} . \tag{A8}$$

The width Γ of the Δ_{33}-resonance and the phase factor ψ_1 are taken according to Eqs. (20) and (30) of Ref. 14.

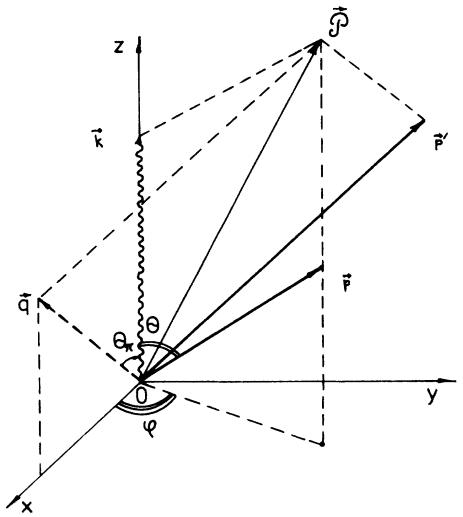

FIG. 6. Pion photoproduction kinematics.

APPENDIX B: PRINCIPAL VALUE INTEGRAL IN EQ. (19)

After separating the singular part of the Green function in Eq. (19) one can write the photoproduction partial amplitude in the following form

$$F^{fi}(q_0) = \mathcal{V}^{fi}(q_0)[1 + iq_0\mathcal{F}'(q_0,q_0)] + \frac{2}{\pi}P\int\frac{d^2dq}{q^2 - q_0^2}\mathcal{F}'(q,q_0)\mathcal{V}^{fi}(q) , \tag{B1}$$

where we have omitted the indices L_π, k, and λ. The regularization of the integrand is easily achieved by adding a zero to (B1) in the form $-P\int(q^2 - q_0^2)^{-1}dq = 0$. Further, we perform the substitution $q = (1+z)/(1-z)$, $z \in [-1,1]$, i.e.,

$$P\int dq \cdots \to 2\int_{-1}^{1}\frac{dz}{(1-z)^2}\cdots = \int_{-1}^{1} dz\, J(z) . \tag{B2}$$

Using the N-point Gauss quadrature with the weights W_j $(1 \le j \le N)$ one finds

$$\mathcal{F}^{fi}(q_0)=\mathcal{V}^{fi}(q_0)+iq_0\mathcal{V}^{fi}(q_0)\mathcal{F}'(q_0,q_0)\left[1+iq_0\frac{2}{\pi}\sum_{j=1}^{N}\frac{J(z_j)W_j}{q_j^2-q_0^2}\right]+\frac{2}{\pi}\sum_{j=1}^{N}\frac{q_j^2J(z_j)W_j}{q_j^2-q_0^2}\mathcal{V}^{fi}(q_j)\mathcal{F}'(q_j,q_0)\ . \tag{B3}$$

APPENDIX C: NUMERICAL INTEGRATION IN EQ. (11)

The integration to be performed below can be simplified by the following choice of the coordinate system (see Fig. 6). The z axis of the coordinate system is taken along the photon momentum $\mathbf{k}$ and the spherical coordinates of the pion momentum $\mathbf{q}$ are chosen as $\varphi_\pi=0$ and θ_π (i.e., $\mathbf{q}$ lies in the (x,z) plane). The choice $\varphi_\pi=0$ is indeed equivalent to the general case and does not influence the result. The azimuthal and polar angles of the momenta $\mathbf{p}$ and $\mathbf{p}'$ are (φ,θ) and (φ',θ'), respectively.

Further, we introduce the decomposition

$$G_\beta=G_\beta^{(1)}+i\lambda G_\beta^{(2)}\sin\varphi,\quad 1\le\beta\le 4\ , \tag{C1}$$

where $G_\beta^{(1,2)}$ depend on $q,\cos\theta_\pi,k,p,\cos\varphi$, and $\sin\theta$. Since we consider only the p-shell transitions, the harmonic-oscillator nucleon radial function is always

$$R_{01}(p)=\left[\frac{8b^5}{3\sqrt{\pi}}\right]^{1/2}p\exp(-\tfrac{1}{2}b^2p^2)\ . \tag{C2}$$

Introducing

$$Z_{LM}\equiv[Y_1(\hat{\mathbf{p}})\otimes Y_1(\hat{\mathbf{p}}')]_{LM}\ , \tag{C3}$$

one observes that $\mathrm{Re}Z_{LM}$ as a function of φ depends only on $\cos\varphi$ and $\mathrm{Im}Z_{LM}$ is proportional to $\sin\varphi$. Since

$$\int_0^{2\pi}f(\cos\varphi)\sin\varphi\,d\varphi=0\ , \tag{C4}$$

we have the result

$$I^{\beta}_{LM_L}=(-)^{1+M_L}\int_0^{2\pi}d\varphi\int_{-1}^{1}d(\cos\theta)\int_0^{\infty}p^2dp[\mathrm{Re}Z_{L,-M_L}G_\beta^{(1)}-\lambda\,\mathrm{Im}Z_{L,-M_L}G_\beta^{(2)}\sin\varphi]R_{01}(p)R_{01}(p')\ . \tag{C5}$$

The optimal quadrature formulas used for the numerical work are

$$\int_0^{2\pi}f(\cos\varphi)d\varphi=\frac{2\pi}{N_\varphi}\sum_{j=1}^{N_\varphi}f(t_j)\ , \tag{C6}$$

where

$$t_j=\cos\left[\frac{(2j-1)\pi}{2N_\varphi}\right] \tag{C7}$$

(Chebyshev integration) and

$$\int_0^{\infty}e^{-p^2}F(p)dp=\sum_{j=1}^{N_p}F(p_j)\omega_j\ , \tag{C8}$$

where p_j are zeros of the Laguerre polynomials and ω_j the corresponding weights. The Gaussian quadrature has been used for the θ integration. In all three integrations we have taken ten integration points. Comparing the numerical results with the analytic ones obtained for the terms linear in $\mathbf{p}$ (and using $\mathbf{p}=-i\nabla$) one concludes that the integration error is of the order 10^{-6} or less.

[1]K. Röhrich, L. Tiator, G. Köbschall, Ch. Reifferscheid, Ch. Schmitt, V. H. Walther, K. Weinand, and L. E. Wright, Phys. Lett. **153B**, 203 (1985).

[2]B. H. Cottman *et al.*, Phys. Rev. Lett. **55**, 684 (1985).

[3]P. K. Teng *et al.* Phys. Lett. B **177**, 25 (1986).

[4]M. Yamazaki, K. Shoda, M. Torikoshi, and O. Sasaki, Phys. Rev. C **34**, 1123 (1986).

[5]R. A. Eramzhyan, M. Gmitro, S. S. Kamalov, and R. Mach, J. Phys. G **9**, 605 (1983).

[6]L. Tiator and L. E. Wright, Phys. Rev. C **30**, 989 (1984).

[7]G. Toker and F. Tabakin, Phys. Rev. C **28**, 1725 (1983).

[8]L. Tiator, J. Vesper, D. Drechsel, N. Ohtsuka, and L. E. Wright, Nucl. Phys. **A485**, 565 (1988).

[9]R. Wittman and N. C. Mukhopadhyay, Phys. Rev. Lett. **57**, 1113 (1984).

[10]M. Gmitro, J. Kvasil, and R. Mach, Phys. Rev. C **31**, 1349 (1985).

[11]M. Gmitro, S. S. Kamalov, and R. Mach, Phys. Rev. C **36**, 1105 (1987).

[12]A. K. Kerman, H. McManus, and R. Thaler, Ann. Phys. (N.Y.) **8**, 551 (1959).

[13]C. Vincent and S. Phatak, Phys. Rev. C **10**, 391 (1974).

[14]I. Blomqvist and J. M. Laget, Nucl. Phys **A280**, 405 (1977).

[15]J. R. Taylor, *Scattering Theory* (Wiley, New York, 1972), pp. 266–269.

[16]R. H. Landau and A. W. Thomas, Nucl. Phys. **A302**, 461 (1978).

[17]R. Mach, Czech. J. Phys. **B33**, 549 (1983).

[18]M. K. Singham and F. Tabakin, Ann. Phys. (N.Y.) **135**, 71 (1981); M. K. Singham, Nucl. Phys. **A460**, 597 (1986).

[19]A. A. Chumbalov and S. S. Kamalov, Phys. Lett. B **196**, 23 (1987).

[20]S. Cohen and D. Kurath, Nucl. Phys. **73**, 1 (1965).

[21]A. M. Bernstein, invited talk at the Seventh Seminar on Electromagnetic Interactions in Nuclei at Low and Medium Energies [Institute of Nuclear Research report, U.S.S.R. Academy of Sciences, Moscow, 1988].

[22]A. N. Saharia and R. M. Woloshyn, Phys. Rev. C **23**, 351

(1981).
[23]J. M. Koch and E. J. Moniz, Phys. Rev. C **27**, 751 (1983).
[24]S. A. Dytman and F. Tabakin, Phys. Rev. C **33**, 1699 (1986).
[25]L. Tiator, private communication.
[26]J. Dubach and W. C. Haxton, Phys. Rev. Lett. **41**, 1453 (1978).
[27]R. A. Eramzhyan, M. Gmitro, T. D. Kaipov, S. S. Kamalov, and R. Mach, in *Proceedings of the Second International Workshop on Perspectives in Nuclear Physics at Intermediate Energies, Trieste, 1985,* edited by S. Boffi *et al.* (World Scientific, Singapore, 1985), p. 228.
[28]Ch. Schmitt, K. Röhrich, K. Maurer, C. Otterman, and V. Walther, Nucl. Phys. **A395**, 435 (1983).
[29]F. Zettle, Ph.D. thesis, Institut für Kernphysik, Mainz, 1983.
[30]A. Lliesenfeld, B. Allerti, D. Eyl, G. Köbschall, A. W. Richter, K. Röhrich, Ch. Schmitt, L. Tiator, and V. H. Walther, Nucl. Phys. **A485**, 580 (1988).
[31]P. Stoler, P. F. Yergin, A. Farah, P. C. Dunn, P. K. A. DeWitt-Huberts, A. Kaarsgaarn, J. Koch, and B. Schoch, Phys. Lett. **143B**, 69 (1984).
[32]A. Kaarsggarn, Ph.D. thesis, NIKHEF, Amsterdam, 1985.
[33]R. L. Huffman, J. Dubach, R. S. Hicks, and M. A. Plum, Phys. Rev. C **35**, 1 (1987).
[34]K. Stricker, H. McManus, and J. Carr, Phys. Rev. C **19**, 929 (1979).